Ionospheric Effects on a Wide Bandwidth Chirp Radar Signal

Dennis L. Knepp
NorthWest Research Associates
301 Webster Street
Monterey, CA 93940
(e-mail: dennis.knepp@nwra.com)

Abstract

This work describes numerical techniques to generate realizations or sample functions of the received, demodulated wide bandwidth signal after two-way propagation through ionized turbulence. These signal realizations include the effect of a structured ionosphere that separates the radar and target. The underlying basis for these realizations of the received radar signal is the solution of the scalar Helmholtz equation for the ionospheric transfer function through the use of a multiple phase screen (MPS) propagation code. The formalism here includes both mean (non-structured) and structured ionization and considers a moving radar target that produces additional Doppler, pulse dilation and contraction, and conditions of filter mismatch.

In the case of ionospheric structure, the MPS code solves the parabolic wave equation and allows for direct computation of realizations of the impulse response function of the ionosphere. The MPS simulation is quite general, and may be applied to problems involving numerous, separated, layers of ionization characterized either statistically by spatially varying electron density power spectra or by deterministic specification of the actual electron density. MPS techniques can handle all levels of ionospheric disturbances from the least severe, where only small phase fluctuations occur, to the most severe case of frequency selective scintillation. For wide bandwidth signals, the MPS code is exercised for many frequencies over the bandwidth of the propagating radar signal to calculate the complete ionospheric transfer function.

In addition to dependence on the propagation channel, the receiver output also depends on the transmitted signal and the receiver characteristics. Here the transmitted signals are assumed to be chirps (linear frequency-modulated pulses). Explicit equations are given to generate realizations of the disturbed signal at several locations in the radar signal processing train. For matched filter processing we give expressions for the received signal immediately after downconversion to baseband (i.e., prior to pulse compression) and at the output of the matched filter. For the case of stretch processing an expression is given for the signal after downconversion and deramping. These analytic expressions include the effects of propagation disturbances on a pulse-by-pulse basis and are easily implemented in software. They provide a mechanism to use MPS calculations of the impulse response function to generate realizations of the radar signal at important places in the receiver processing chain.

Such realizations are useful for numerical simulation and hardware testing of radars that must operate under disturbed propagation conditions, for example HF through UHF radar in the natural equatorial or polar region. Several useful examples are presented that illustrate the effects of time- and frequency-selective ionospheric fading on demodulated chirps.

Channel Description

This section describes the ionospheric channel for propagation in both the mean and the disturbed ionosphere. The two-way radar channel model here is partially described in *Knepp and Brown* [1997]. First consider a propagation channel with a non-time-varying ionosphere and fixed range to the radar target. The scalar Helmholtz equation for a propagating wave can be written as follows [*Yeh and Liu*, 1977].

$$\nabla^2\psi + k^2 n^2(1+\gamma\epsilon)\psi \;=\; 0 \tag{1}$$

where

$$n^2 = 1 - \frac{f_p^2}{f^2}; \quad \gamma = \frac{f_p^2}{f_p^2 - f^2}; \quad \epsilon = \frac{\Delta N_e}{\langle N_e\rangle} \tag{2}$$

and f is the transmission frequency in units of Hertz, $f_p^2 = c^2 r_e\langle N_e\rangle/\pi$, where f_p is the plasma frequency, r_e is the classical electron radius, $\langle N_e\rangle$ is the mean electron density, and ΔN_e is the deviation in electron density due to small scale structure. Here the time dependence $\exp(i\omega t)$ is suppressed, where $\omega = 2\pi f$. The symbol k is the wavenumber and c is the speed of light in a vacuum, $k = 2\pi f/c$.

The solution to (1) can be expressed as the product of two components where one is the solution for $\epsilon = 0$ and the other is the solution of the parabolic wave equation [*Yeh and Liu*, 1977]. Let the index of refraction, n, be a function only of z and assume that there is no small scale ionospheric structure, so that $\epsilon = 0$. The plane wave solution for one-way propagation from 0 to z is easily found as

$$T_{\mathrm{mean}}(f,z) \;=\; \exp\left\{-ik\int_0^z n(z')\,dz'\right\} \tag{3}$$

provided that the derivative of n with respect to z is small. Reconsider the full equation (1) and write the solution as the product $T_1(x,y,z,f) = T_{\mathrm{mean}}(f,z)T_{\mathrm{struct}}(f,x,y,z)$. Inserting this expression into (1) gives the parabolic wave equation for T_{struct} with the usual provision that the structure scale size is much larger than the wavelength,

$$\frac{\partial^2 T_{\mathrm{struct}}}{\partial x^2} - 2ik\frac{\partial T_{\mathrm{struct}}}{\partial z} + 2k^2\Delta n(x,z,\omega)T_{\mathrm{struct}} = 0 \tag{4}$$

For ionization irregularities $\Delta n = -r_e\lambda^2\Delta N_e/2\pi$. In writing (4) it is assumed that the irregularities are infinite in length and aligned along the y-direction. This geometry is a good model of transionospheric propagation near the equator.

Now separate the ionized region into a number of thin layers, each of which is modeled as a central phase changing screen (phase screen) surrounded by free space. Consider a layer of thickness Δz centered at zero z. For small Δz the equation for propagation through this layer is obtained from (4) with the first (diffraction) term neglected. The solution is

$$T_{\mathrm{struct}}\left(x, \frac{\Delta z}{2}, \omega\right) = T_{\mathrm{struct}}\left(x, -\frac{\Delta z}{2}, \omega\right)\exp\left\{-ik\int_{-\frac{\Delta z}{2}}^{\frac{\Delta z}{2}} \Delta n(x,z',\omega)dz'\right\} \tag{5}$$

The exponential term is simply the geometric optics phase change after straight line propagation. Equation (5) handles propagation through the phase screen.

Equation (4) is valid for free-space propagation between the phase screens if the last term is neglected. The resulting equation is solved by Fourier transform, giving

$$T_{\mathrm{struct}}(x,z_2,\omega) = \int_{-\infty}^{\infty} \hat{T}_{\mathrm{struct}}(q,z_1,\omega)\exp\left[i2\pi^2q^2(z_2-z_1)/k + i2\pi qx\right]dq \tag{6}$$

where

$$\hat{T}_{\text{struct}}(q,z,\omega) = \int_{-\infty}^{\infty} T_{\text{struct}}(x,z,\omega)\exp(-i2\pi qx)dx \tag{7}$$

The solution for the electric field is then obtained using (5) and (6), propagating from screen to screen and finally to the receiver plane. The numerical solution to the parabolic wave equation using multiple phase screens is discussed in *Knepp*, [1983] for plane waves and in *Knepp*, [2015] for spherical waves.

The multiple phase screen code calculates realizations of the function $T_{\text{struct}}(x,f)$, which is transformed to $T_{\text{struct}}(t,f)$ through the assumption of some velocity at which the phase screen moves past the receiver.

For two-way radar propagation, the channel impulse response function is the Fourier transform of the transfer function as specified through the expression

$$T(t,f) \;=\; \int h(t,\tau)e^{-i2\pi f\tau}\,d\tau\text{–trans-func} \tag{8}$$

The results here also require the function $G(\nu,\tau)$ that *Bello* [1963] calls the Doppler-delay-spread function

$$G(\nu,\tau) \triangleq \int h(t,\tau)e^{-i2\pi\nu t}\,dt\text{–Htrans-1} \tag{9}$$

In the following, multiple integrals are generally written with a single integral sign and the (unwritten) limits are from negative to positive infinity.

Received waveform

Now suppose that the transmitted signal is a pulse train, modulated on a carrier f_0, of the form

$$x(t) = \sum_n s(t-nT_p)e^{i2\pi f_0 t}\text{–train} \tag{10}$$

where n is the pulse number, T_p is the time between pulses, and $s(t)$ is referred to as the baseband pulse. The received signal after two-way propagation is found to be

$$\begin{aligned} z(t) \;&=\; e^{i(2\lambda_0 r_e N_t - 2k_0 r)}\sum_n \int h(t,\tau)s(\beta(t-t_0)-\tau-nT_p-2\tau_I)e^{-i2\pi f_0\tau}d\tau \\ &\quad\times e^{i2\pi(f_0+f_{dop})(t-t_0)-i2\pi f_0(2\tau_I)}\text{–rec-sig} \end{aligned} \tag{11}$$

In (11) $\lambda_0 = c/f_0$, N_t is the total electron content along the two-way propagation path, $\beta = (c-\dot{r})/(c+\dot{r})$, $\dot{r}$ is the range rate of the radar target, t_0 is the time-delay due to two-way free space propagation, τ_I is the one-way time delay due to mean ionization, and $f_{dop} = -2\dot{r}f_0/(c+\dot{r})$ is the target Doppler shift. For the case of constant range, a mean ionosphere with no dispersion, and no random structure so that $T_{\text{struct}}(f) = 1$, (11) becomes the familiar

$$z(t) = e^{i(2\lambda_0 r_e N_t - 2k_0 r)}s(t-t_0-2\tau_I)e^{i2\pi f_0 t}\text{–rec-sig} \tag{12}$$

Transmitted chirp waveform and matched filter

Here we consider the effects of structured ionization on a received chirp pulse. Many modern long-range radars transmit linear frequency modulated signals (chirps) because of simplicity of pulse generation and the desire for high range resolution together with high received signal-to-noise ratio (SNR) [*Klauder, et al.,* 1960]. In this case the transmitted signal at baseband is

$$\begin{aligned} s(t) &= u_T(t)s'(t)\text{–eq:unitimpulseandsoft} & (13) \\ &= u_T(t)e^{+i\pi\alpha t^2}\text{–eq:ChirpSignalTwo} & (14) \end{aligned}$$

where u_T is a unit rectangle of duration T, $u_T(t) = 1, -T/2 \leq t \leq T/2$, and $\alpha = \pm B/T$ is the chirp slope. B is the chirp bandwidth and T is the uncompressed pulse duration. For $\alpha > 0$ the instantaneous frequency of the transmitted baseband pulse ranges from $-B/2$ to $B/2$ during the pulse duration. High SNR is obtained at the output of the matched filter through the process of pulse compression wherein a delay-equalizing filter is applied to properly delay the earlier portions of the arriving signal so that they coherently add to the later portions of the signal.

Upon reception, downconversion to baseband is accomplished by multiplication of the received signal, $z_b(t) = z(t)\exp(-i2\pi f_0 t)$. Pulse compression may then be accomplished by multiplication of the downconverted waveform by a matched filter. The output of the matched filter is given by

$$o(t) = \int z_b(t')m(t-t')\,dt'\text{–mf6} \qquad (15)$$

where $m(t) = s^*(-\beta' t)w(t)$. The function $w(t)$ represents a time-domain weighting function commonly applied to reduce range sidelobes. The factor β' is the receiver estimate of β, based on the current estimate of target range rate.

After much algebra, the compressed chirp produced from matched filter processing can be written as

$$\begin{aligned} o(t) &= e^{i\pi f_{dop}^2/\alpha} \int E_{bb}(\tau')Q(t'-\tau')e^{-i\pi f_{dop}(t'-\tau')}\,d\tau' \\ &\quad \times e^{i2\pi f_{dop}t}e^{-i2\pi(f_0+f_{dop})t_0}\text{–o-convol2} & (16) \end{aligned}$$

where

$$\begin{aligned} t' &= t - t_0 - nT_p' + f_{dop}/\alpha & (17) \\ E_{bb}(\tau) &\triangleq \beta \int G_{bb}(\nu, \beta(\tau+\nu/\alpha))e^{i2\pi\nu(t_0+nT_p')}\,d\nu\text{–Hbbp-def1} & (18) \end{aligned}$$

and G_{bb} is a simply a frequency-shifted version of G given by (9), i.e., $G_{bb}(\nu,\tau) = e^{-i2\pi f_0\tau}G(\nu,\tau)$. The function Q is related to the ambiguity function and is defined by

$$Q(t+f/\alpha) = u_{2T}(t)\,\frac{\sin\pi T(f+\alpha t)}{\pi(f+\alpha t)}\text{–X-sin} \qquad (19)$$

This important result states that if we have a realization of the two-way radar channel impulse response function $h_{bb}(t,\tau)$, or equivalently its transform $G_{bb}(\nu,\tau)$, we can generate realizations of the received, compressed signal $o(t)$ through a single convolution. The two terms that are convolved are the matched filter response in the absence of multipath, $Q(t)$, and the term $E_{bb}(\tau)$. The term $E_{bb}(t)$ is the Fourier transform of the Doppler-delay-spread function that describes the two-way radar channel and is obtained by sampling $G_{bb}(\nu,\tau)$ along a straight line in $\nu - \tau$ space.

Scattering from a homogeneous ionosphere

In the following examples, we use a homogeneous multiple phase screen calculation to provide the propagation environment. Here ten phase screens are used to model a 420-km thick ionosphere. Each phase screen has a q^{-3} power-law power spectral density with outer scale of 10 km and inner scale of 10 m. The phase standard deviation of each screen is chosen as 15.8 radians. The transmission center frequency is 300 MHz and the 40-MHz bandwidth has 128 frequency components ranging discreetly from -280 to 319.7 MHz. The one-way propagation geometry corresponds to a plane wave incident on the 420-km thick ionosphere and then propagating an additional 420 km to the receive plane on the ground. The phase screen consists of $2^{17} = 131,072$ points with a 100 km grid length. This length corresponds to a total wall-clock time duration of 1000 seconds using 100 m/sec as the assumed line-of-sight velocity. Figure 1 shows one of the phase screens as a function of wall-clock time along the entire MPS grid.

We analyzed the output of the MPS calculation to obtain several statistical quantities that characterize propagating waveforms, namely the scintillation index and the signal decorrelation time. Both of these quantities are obtained from the spectral component of the transfer function at the carrier frequency, 300 MHz. The scintillation index is the standard deviation of the power normalized by the mean power and is 1.15 for the realization generated for this example. The signal decorrelation time (τ_0) is defined at the $1/e$ point on the magnitude of the autocorrelation function of the complex received signal and is here 0.629 seconds. The coherence bandwidth refers to the bandwidth within which the spectral components are correlated. For this MPS calculation, the theoretical coherence bandwidth is 22.3 MHz. We did not measure this quantity in the calculation. For chirp pulses whose duration exceeds the decorrelation time, the matched filter output will experience degradation including loss of peak power and multiple sidelobes in the range (or fast-time) dimension. For radar chirps with bandwidth greater than the coherence bandwidth, somewhat similar effects will occur. Knepp and Brown, [1997] describe these effects in terms of the average received pulse shape, but not to the level of detail considered here.

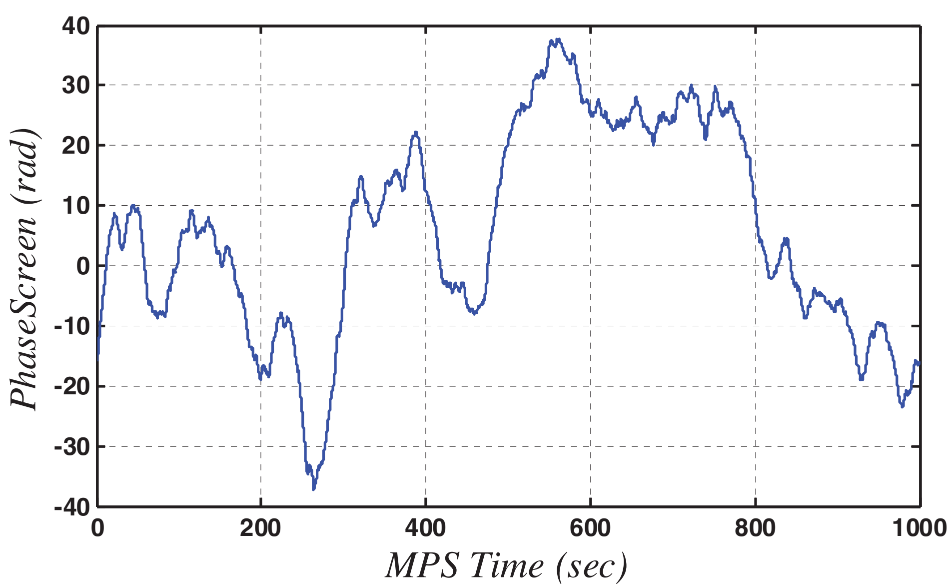

Figure 1: One of the ten phase screens used to model a thick homogeneous ionosphere.

Frequency-flat fading

Frequency flat fading occurs when all the frequency components across the signal bandwidth experience the same propagation disturbance. Figure 2 (top-left) shows the amplitude and phase of the ionospheric channel at the center frequency of 300 MHz. Only a short portion, of duration 10 seconds, of the entire MPS calculation grid is shown for this example of flat fading. Figure 2 (top-right) shows the magnitude of the channel transfer function over the 10-second period. To create an example of frequency flat fading, we set all the frequency components of the transfer function to their values at the center frequency. In the next example, we utilize the calculated transfer function without modification.

Figure 2 (bottom-left) shows 100 realizations of the received chirp waveform for the case of a transmitted signal with a time duration, T of 0.04 seconds and a chirping bandwidth of 40 MHz. The duration of the chirp pulse here is much smaller than τ_0, so there is no possibility for time selective fading. The received signal amplitude is shown as a series of pulses plotted one behind the other in the figure, over a small portion of the MPS calculation. The pulses are spaced by about 0.1 seconds in wall-clock time. For this case of flat fading, all the received pulses retain the same shape but their amplitude is affected by the amplitude of the ionospheric transfer function.

Frequency-selective scintillation

Figure 2 (bottom-right) shows an example of the effects of frequency selective ionospheric fading on 100 received pulses over the time interval from 10 to 20 seconds in the MPS calculation. The transmitted chirp pulse duration is 0.04 seconds and the bandwidth is the entire frequency extent of the MPS calculation, 40 MHz. For this calculation, the amplitude of the ionospheric transfer function as a function of frequency and distance is shown in Figure 2 (top-right). The primary difference between the calculations underlying Figures 2 (bottom-left) and 2 (bottom-right) is that the latter calculation uses all the frequency components of the transfer function shown in Figure 2 (top-right).

In Figure 2 (bottom-right) the received pulses are distorted in their trailing edges only, in the direction of increasing range delay, to the right in the figure. The leading edges (to the left in the figure) experience a little time-delay jitter and amplitude fading, but the shape of the leading edge of the pulse is not affected. This behavior is similar to that shown above in the examples describing scattering from a structured barium cloud. This behavior occurs because ionospheric scattering always delays (never advances) various components of the propagating wave. The delayed components arrive at the receiver at later times (depending on the amount of the delay) and interfere with other delayed components. The amount of the delay depends on the angle over which the wave is scattered, which is a function of the frequency within the signal bandwidth.

References

Klauder, J. R., A. C. Price, S. Darlington, and W. J. Albersheim (1960), "The theory and design of chirp radars," *Bell Sys. Tech. J., 39 (4)*, 745-808.

Knepp, D. L. (1983), "Multiple Phase-Screen Calculation of the Temporal Behavior of Stochastic Waves," *Proceedings of the IEEE*, *71*, No. 6, pp. 722-737, June 1983.

Knepp, D., and W. Brown (1997), "Average received signal power after two-way propagation through ionized turbulence,," *Radio Sci.*, *32(4)*, 1575-1596.

Knepp, D. L. (2016), "Multiple phase screen calculation of two-way spherical wave propagation in the ionosphere," *Radio Sci.*, 51, 259270, doi:10.1002/2015RS005915.

Yeh, K. C., and C. H. Liu (1977), "An investigation of temporal moments of stochastic waves," *Radio Sci.*, 12(5), 671680, doi:10.1029/RS012i005p00671.

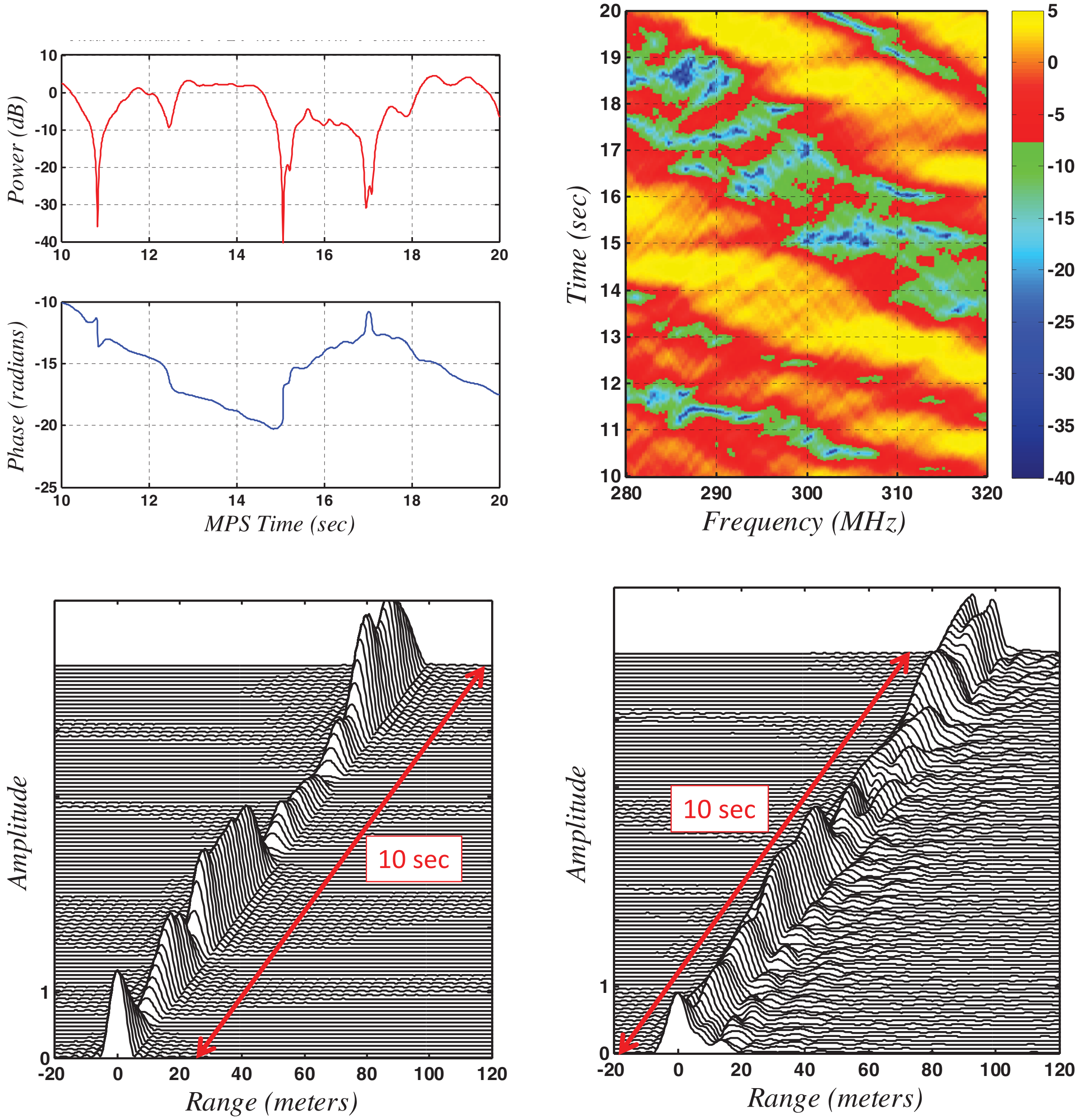

Figure 2: Top left: Amplitude and phase of channel at f_0. Top right: Amplitude in dB of the ionospheric transfer function. Bottom left: Example of flat fading. Bottom right: Frequency-selective fading.